International Journal of Thermophysics, Vol. 10, No. 6, 1989

Molecular Dynamics of Stage 3 Cesium Intercalated Graphite $C_{36}Cs$

P. A. Wielopolski[1] and J. W. White[1]

Received February 15, 1989

Stage 3 casium intercalated graphite is simulated. The dependence of the structural properties of the simulated system on the barrier height of the graphite periodic potential is shown. The periodic component of the radial distribution function $g(r)$ due to the substrate modulation potential is clearly visible. It appears as a result of the delicate balance between the in-plane cesium–cesium interactions and the substrate modulation potential.

KEY WORDS: cesium; computer simulations; intercalation; molecular dynamics; radial distribution function.

1. INTRODUCTION

Intercalation compounds are formed by the insertion of atomic or molecular layers of a guest species—an intercalant—between layers in a host material. Graphite is a good example of a host material for intercalation compounds. After graphite is exposed at elevated temperatures to the vapor phase of either alkali metals or a variety of molecular species, the normal sequence of graphite layers is regularly interrupted by single layers of an intercalent. The stage of intercalation is defined as a number of graphite layers separating layers of intercalated species.

The intercalated layers present a quasi two-dimensional (2D) system subjected to the (a) periodic potential due to the graphite lattice and (b) out-of-plane intercalant–intercalant interactions, the latter depending strongly on the stage of intercalation. The static and dynamic properties of an intercalated layer are determined by the competition of inter- and

---

[1] Research School of Chemistry, The Australian National University, Canberra 2601, Australia.

intralayer interactions with those of the potential energy surface due to the graphite lattice.

In this paper we neglect the interlayer interactions, which are negligible for stage 3 compounds at higher temperature. We report molecular dynamics simulations of cesium intercalated graphite in stage 3. Our concern is the structure of a 2D layer of cesium atoms in the periodic field due to the graphite lattice at temperatures near 300 K, where quasi liquid behavior has been observed for the alkali metal layer [1]. As in our previous papers [2–4] the periodic potential is modeled via Lennard–Jones interactions between cesium and carbons of the graphite lattice. In this work we chose the potential parameters to give a barrier height of 0.0585 eV (rather lower then estimates from X-ray analysis [5] but consistent with calculations based on the density functional theory [6]). The primary objective of this paper is to compare the structure of the intercalated layer calculated with this barrier height to our previous results from a barrier height of 0.0338 eV. The anisotropy of the system induced by the modulation potential is briefly discussed.

Section 2 describes briefly the potential models and details of the simulations. Results of the simulations are presented and discussed in Section 3.

2. POTENTIAL AND SIMULATION DETAILS

The potential used in the simulations has been described previously [2]. It consists of a two-dimensional periodically varying one-body potential, $U^{(1)}$, due to the interactions of the cesium atoms with the graphite lattice; the Lennard–Jones parameters of the cesium–graphite interactions are taken as $\varepsilon/k = 150$ K and $\sigma = 3.24$ Å.

The interactions between cesium atoms are composed of two parts [2]: (i) a Lennard–Jones interaction, $U_{\mathrm{L-J}}$, with $\varepsilon/k = 190$ K and $\sigma = 3.61$ Å, between Cs^+ cores, and (ii) an electrostatic interaction, $U_{\mathrm{Q-Q}}$, modeled by rigid axial quadrupoles perpendicular to the graphite layers.

The electrostatic part approximates the screening due to the readjustment of the conduction electron distribution according to the motion of ion cores. Thus, the potential used in simulations is of the form

$$U(\{r^N\}) = \sum_i U^{(1)}(r_i) + \sum_{i<j} [U_{\mathrm{Q-Q}}(r_i, r_j) + U_{\mathrm{L-J}}(r_i, r_j)] \qquad (1)$$

The geometry of the graphite lattice corresponds to normal graphite; the nearest in-plane neighbor distance is 1.42 Å and the nearest interplane distance is 3.35 Å. The distance between graphite planes confining the cesium layer was taken equal to 6.01 Å, the experimentally measured value [7].

The graphite modulation potential has been calculated for a set of points and was used in the form of a table during the simulations. The values of forces and energy between the calculated positions were obtained by linear interpolation. The motion of the ion cores was restricted to the plane midway between two adjacent graphite planes and no rotations of axial quadrupoles were allowed.

The MD simulations were performed with 576 Cs atoms, and the planar density of Cs corresponded to that of a stage 3 compound with the bulk stoichiometry $C_{36}Cs$; thus, the ratio of the number of cesium atoms to the number of carbon atoms in the adjacent carbon layer is 1:12. The minimum image boundary conditions were imposed on the system and the cutoff distance for the interactions has been taken equal to $18.4\,\sigma$ ($\sigma = 3.61$ Å). The simulation box is a rectangle rather than a square. For a given number of simulated atoms there are a few possible choices of the box side lengths accommodating the periodicity of the graphite lattice. We chose the one for which the box side length ratio is closest to one. Newton's equations of motion were integrated with the Verlet algorithm [8]. The time step of integration was 0.009 ps and the run extended to 21,000 ts. The calculations were performed on a Fujitsu VP(100) supercomputer.

3. RESULTS AND DISCUSSION

The average temperature of the MD run was 292.4 K. During simulations the histograms were accumulated for calculations of the time-independent properties, namely, the radial distribution function, $g(r)$, density profiles, $n(x)$ and $n(y)$, and the planar probability density, $p(r)$, of finding a cesium atom at a given distance from the center of a graphite hexagon. The static structure factor $S(\mathbf{k})$ was calculated in the $\mathbf{k}$ vector-dependent form and averaged over all vectors $\mathbf{k}$ having a length between k and $k + \Delta k$.

The results of the present simulations (referred to as system A below) are compared with those performed with 192 Cs atoms [4] for the barrier height of 0.0338 eV (system B; the efficiency of the then accessible MicroVax computer limited out calculations to 192 cesium atoms). We have verified that, in this context, the effects of system size are insignificant.

3.1. Structural Properties

A convincing illustration of the anisotropy induced in system A is presented in Fig. 1. The singlet density distribution function is plotted as

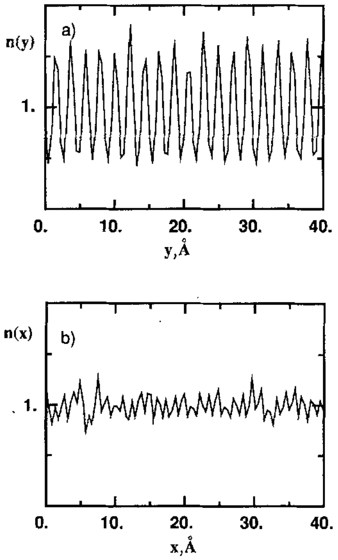

Fig. 1. Profiles of the singlet density distribution function for system A; $n(x) = n(y) = 1$ corresponds to the isotropic distribution.

viewed along the x and y directions of the graphite lattice. The lattice structure is reflected in the different periodicities of the two cuts. The distance between the consecutive peaks of $n(y)$ is equal to 2.13 Å, which corresponds exactly to the distance between hexagon centers viewed from the y direction. The curves are not as well formed as those obtained for the system treated by the self-consistent solution of integral equations [9] with about 1.5 times stronger graphite potential, but the essential lattice periodicity is apparent. Results for the density profiles of system B are very similar but the amplitude of the oscillations is lower.

In Fig. 2 the radial distribution functions are presented. The $g(r)$ for system A (Fig. 2a) clearly displays the competition resulting from different length scales defined by the size of Cs atoms and the periodicity of the underlying potential. At short distances the Cs–Cs interactions dominate the shape of $g(r)$; at large r the long-range periodic component prevails. The $g(r)$ of system B (Fig. 2b, thick line) looks much more “liquid-like”; the periodic component is hardly visible. We have shown in Ref. 4 that it is practically undistinguishable from the “real” liquid $g(r)$ obtained with the graphite periodic potential equal to zero.

Both the singlet distribution function (Fig. 1) and the $g(r)$ (Fig. 2a) of

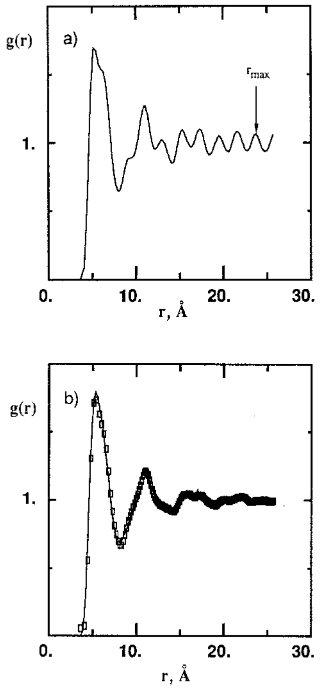

Fig. 2. Radial distribution functions. (a) System A, modulated $g(r)$. (b) Solid line, $g(r)$ of system B; open squares, "unmodulated" $g(r)$ of the system A.

system A show the existence of a pronounced density wave induced by the increased barrier height of the periodic potential. If the structure represented by $g(r)$ is a simple response to the increase in the barrier height, then the extraction of the periodic component from system A's $g(r)$ should lead us back to the $g(r)$ of system B. To extract the periodic component from the $g(r)$ of system A we make use of the fact that the periodic modulation of $g(r)$ gives rise to a δ-function Bragg contribution to the static structure factor $S(k)$ at the reciprocal vectors of the graphite lattice. The $S(k)$ values for system A and system B are displayed in Fig. 3. The cosine wave with a period λ, defined by the position of the δ function in $S(k)$ $k_g = 2\pi/\lambda = 2.945\ \text{Å}^{-1}$, and an amplitude a estimated from $g(r)$ at large r is taken away from system A's $g(r)$. The procedure is as follows: the position of a maximum of $g(r)$ at a large r is found and denoted $r_{\max}$ (see Fig. 2a), then the equation $k_g r_{\max} + \theta = (2n+1)\pi$ is solved for a phase shift θ and the

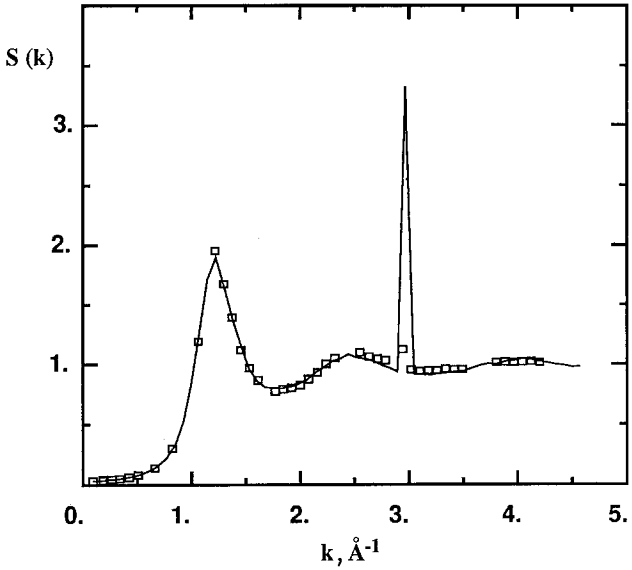

Fig. 3. Structure factor $S(k)$ averaged over angles. Solid line, system A; open squares, system B.

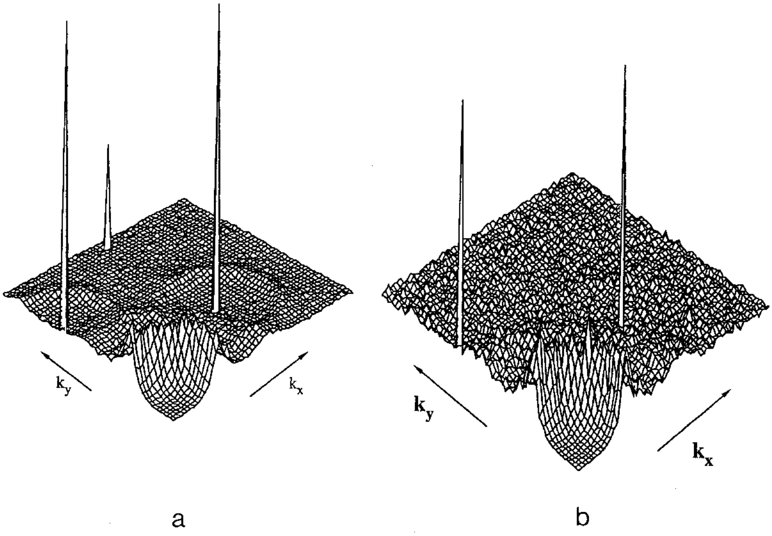

Fig. 4. The structure factor $S(\mathbf{k})$ in the first quadrant as a function of k_x and k_y. (a) System A, with the intensities of the twop main Brag peaks reduced by a factor of 8 and the third one by a factor of two; (b) system B, with Bragg peaks of normal intensity.

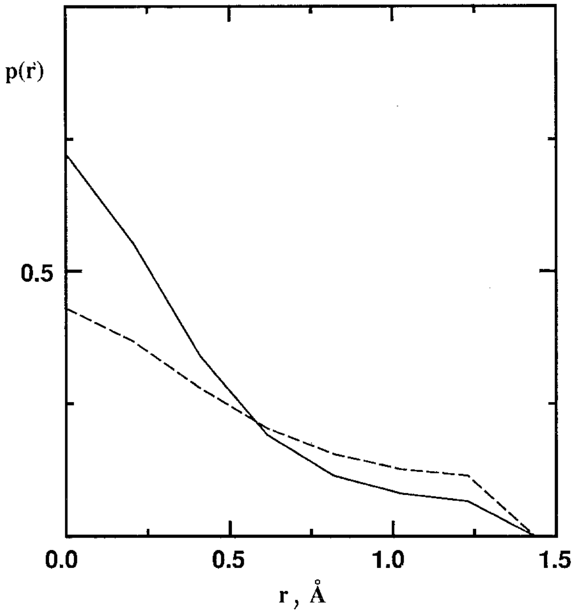

Fig. 5. The planar probability function $p(r)$. Solid line, system A; dashed line, system B.

"unmodulated" $g(r)$ (dnoted by open squares in Fig. 2b) is found by addition: $g_{\text{unmod}}(r) = g_{\text{mod}}(r) + a\cos(k_g r + \theta)$. As may be seen in Fig. 2b, the unmodulated $g(r)$ of system A matches perfectly well that of system B.

Thus, the strong periodic potential introduces a solid-like component into the system, causing the increased registration of the cesium atoms.

Perhaps the most spectacular presentation of this result is that of the calculated $S(\mathbf{k})$ shown for the first quadrant in **k** space in Fig. 4. The sixfold symmetry, corresponding to that of the underlying lattice, is quite evident. The sharp spikes at the reciprocal vectors of the graphite lattice, together with their surrounding halos, were experimentally observed in X-ray scattering experiments on $C_{24}Rb$ and $C_{24}K$ [10, 11]. The much more intense spikes of system A indicate stronger localization of the Cs atoms at the centers of the graphite hexagons. This result may be seen as well in Fig. 5, where the probability of finding a Cs atom at a given distance from the center of a hexagon is plotted.

3.2. Concluding Remark

The strong influence of the strength of the graphite periodic potential on the structure of the intercalated layer is evident from Figs. 2–5. Our simulations show that for a barrier height of 0.0585 eV and temperature $T = 291$ K, the intercalated layer of cesium atoms may be regarded as a strongly modulated liquid phase. It seems very possible that further increase in the barrier height may cause a phase transition to a registered state. Work on this subject is in progress.

ACKNOWLEDGMENTS

We are grateful to the Computer Services Centre of the Australian National University for a computing time on the Fujitsu VP-100 supercomputer. One of us (P.A.W.) acknowledged financial assistance from the organizers of the Tenth Symposium on Thermophysical Properties. We are grateful for some valuable discussions with H. J. M. Hanley.

REFERENCES

1. R. Clarke, N. Caswell, S. A. Solin, and P. M. Horn, *Phys. Rev. Lett.* **43**:2018 (1979).
2. J. W. White and P. A. Wielopolski, *Phys. Rev. B* **36**:6069 (1987).
3. J. W. White and P. A. Wielopolski, *Mol. Phys.* **63**:165 (1988).
4. J. W. White and P. A. Wielopolski, *Mol. Phys.* **63**:669 (1988).
5. S. C. Moss, G. Reiter, J. L. Robertson, C. Thompson, and J. D. Fan, *Phys. Rev. Lett.* **57**:3191 (1986).
6. D. P. DiVincenzo and E. J. Mele, *Phys. Rev. B* **22**:2538 (1985).
7. W. Stead, Ph.D. thesis (Oxford, University, Oxford, 1986).
8. L. Verlet, *Phys. Rev.* **1259**:98 (1967).
9. O. A. Karim and B. M. Pettitt, *Chem. Phys. Lett.* **137**:72 (1987).
10. F. Rousseaux, R. Moret, D. Guerard, P. Lagrange, and M. Lelaruain, *J. Phys. (Paris) Lett.* **45**:L111 (1984).
11. F. Rousseaux, R. Moret, D. Guerard, P. Lagrange, and M. Lelaruain, *Synth. Met.* **12**:45 (1985).